# Structural Performance Evaluation of Segmented Wind Turbine Blade through Finite Element Simulation

Chandrashekhar Bhat, Dilifa J. Noronha, Faber A. Saldanha

*Abstract*—Transportation of long turbine blades from one place to another is a difficult process. Hence a feasibility study of modularization of wind turbine blade was taken from structural standpoint through finite element analysis. Initially, a non-segmented blade is modeled and its structural behavior is evaluated to serve as reference. The resonant, static bending and fatigue tests are simulated in accordance with IEC61400-23 standard for comparison purpose. The non-segmented test blade is separated at suitable location based on trade off studies and the segments are joined with an innovative double strap bonded joint configuration. The adhesive joint is modeled by adopting cohesive zone modeling approach in ANSYS. The developed blade model is analyzed for its structural response through simulation. Performances of both the blades are found to be similar, which indicates that, efficient segmentation of the long blade is possible which facilitates easy transportation of the blades and on site reassembling. The location selected for segmentation and adopted joint configuration has resulted in an efficient segmented blade model which proves the methodology adopted for segmentation was quite effective. The developed segmented blade appears to be the viable alternative considering its structural response specifically in fatigue within considered assumptions.

*Keywords*—Cohesive zone modeling, fatigue, segmentation, wind turbine blade.

## I. INTRODUCTION

THE primary factors which governs the wind turbine development are, power generation and cost. Considering no changes in design, materials or construction methods, the power output increases with blade length which drives the recent trend of increase in wind turbine blade sizes. It is observed that, during the last three decades wind turbine rotors have grown in sizes from a 15m diameter to over 125m and in future, they are expected to rise beyond 250m [1]. With increase in blade sizes, wind turbine industry is facing stern structural challenges along with increased difficulties in manufacturing, handling, haulage and assembly. Dayton Griffin [2] in his work concludes that, increase in haulage costs is almost an inevitable consequence for large blades. Irrespective of the design scenarios, the increase in mass at cubic rate with blade length is also observed which augment the handling difficulty. Novel materials may address the

problems arising with increased mass; however, an efficient solution for managing size aspects is still an engineering challenge. Considering the shipment, handling and assembly are of paramount importance, a concept of "*Segmented Blades*" where in the blades are manufactured as smaller segments and assembled on-site through suitable arrangements is believed to be the feasible alternative.

In recent past, many segmentation techniques have been proposed which shows that, developing innovative segmented blades is a tough challenge [3]-[13]. Most of the work related to segmentation of wind turbine blades is found to be patented [6]-[11] and only a small portion of it is available in public domain. However, published work does exist, which indicates that, an efficient design of segmented blade still remains to be an engineering problem. Reliability of a segmentation concept in fatigue is one of them, which is considered to be a multi-disciplinary problem. The need of further research in this domain is observed. Identifying a suitable location for segmentation and designing a joint to fasten the segments are the two critical issues encountered in the design of an efficient segmented rotor blade. Literatures show that, the resonant characteristics (natural frequency and mode shapes) and static displacement as a function of blade length can be considered as the primary parameters for selecting a suitable location for segmentation [3], [14]-[16]. A double strap bonded joint configuration is observed to be the novel concept for joining the blade segments. Cohesive Zone Modeling (CZM) approach is identified to be the widely used technique for analyzing the bonded joint behaviors [17], [18].

Every new blade design must be evaluated for its structural integrity, load carrying capability and service life which make the investigation on structural behaviors crucial in the development process of segmented blades. The resonant, static, and fatigue performances are identified to be the crucial parameters in the validation of a segmented blade concept. From the literature it is evident that, the aerodynamic loads which causes flap wise bending of the blade are critical from structural standpoint [19]-[21]. It is also noted that, the evaluation procedure required for segmenting a rotor blade must be validated through fatigue criteria. K. Vellons et al. [22] states that, nearly 25% of the turbine failures occur due to rotor breakdown under fatigue and emphasize the need for fatigue testing of rotor blades. F. A. Saldanha et al. [3] proposed an evaluation procedure for segmenting a wind turbine blade which is to be checked for its reliability under fatigue.

Further, the developed segmented blade must conform to the performance of non-segmented blade for commercial

Chandrashekhar Bhat is with the Department of Mechatronics Engineering, Manipal Institute of Technology, Manipal, India, 576104 (e-mail: chandra.bhat@manipal.edu).

Dilifa J. Noronhna is with the Department of Mechanical and Manufacturing Engineering, Manipal Institute of Technology, Manipal, India, 576104 (Phone: +91-9916-528-988; e-mail: dj.noronha@manipal.edu).

Faber A. Saldanha is formarly with the Manipal Institute of Technology, Manipal University, Manipal, India, 576104 (e-mail: fabersaldanha@yahoo.com).

World Academy of Science, Engineering and Technology
International Journal of Mechanical and Mechatronics Engineering
Vol:9, No:6, 2015

utilization. Thus, development of a feasible segmentation technique and detail investigation of the structural performance is required. It may be achieved through finite element simulation method, so that an engineering solution can be obtained to reduce the difficulties in producing segmented rotor blades. In the present work an attempt has been made to address this requirement by investigating the structural performances of a horizontal axis wind turbine blade subjected to static and fatigue loading, to develop a prospective segmented wind turbine blade model.

## II. METHODOLOGY

The methodology presented here is used to develop a segmented wind turbine blade and simulate the performance tests in accordance with IEC61400-23 standard [23]. The resonant, static bending and fatigue tests are simulated to check for its structural integrity, load carrying capability and fatigue damage distribution.

### A. Procedure

The process adopted in the design and testing of segmented blade involves following steps;

- Developing a non-segmented wind turbine blade model in accordance with the guidelines provided for rotor blade design.
- Testing the developed rotor blade to check for resonant, static and fatigue behaviors through finite element simulation method as per IEC-61400-23 standard. These performances serve the purpose of reference for comparison.
- Splitting of single piece test blade at suitable location based on specific segmentation technique and joining the modules through suitable joining technique.
- Testing the developed segmented blade for resonant, static and fatigue behaviors through finite element simulation.
- Comparing and investigating the structural response of non-segmented and segmented wind turbine blades.

### B. Selection of Blade Material

The basic design process for a turbine blade also involve selection of optimum material which should be stiff, strong, light, durable and cost effective. In the present work, this is achieved through TOPSIS (Technique for Order Preference by Similarity to Ideal Solution) method which is a MCDM (Multiple Criteria Decision Making) technique [24].

By trade off studies [25], [26] we observed that, the optimum material chosen for wind turbine blade must possess high material stiffness, high strength, low density for better performance and low cost to make the blade affordable. Based on these requirements, the materials and their properties selected for comparison are listed in Table I.

The solution obtained through TOPSIS method for the materials compared is presented in Table II. The optimum material must have its relative closeness index, closer to unity which is the ideal solution. From Table II, E-glass/Epoxy has

the closest value to the ideal solution. Thus, it is selected as the best material for the blade within considered assumptions.

TABLE I
MATERIALS AND THEIR PROPERTIES ASSUMED FOR COMPARISON

| Material | Stiffness | Tensile Strength | Density | Cost/Kg |
|---|---|---|---|---|
| | GPa | MPa | kg/m³ | ₹ |
| Steel | 30 | 190 | 7500 | 81 |
| Aluminium | 10 | 90 | 2700 | 384 |
| E-Glass/Epoxy | 38 | 1800 | 1870 | 229 |
| Carbon/Epoxy | 176 | 2050 | 1490 | 6820 |
| Aramid/Epoxy | 61 | 1850 | 1330 | 3720 |

TABLE II
RELATIVE CLOSENESS OF MATERIALS TO THE IDEAL SOLUTION

| Material | Relative Closeness Index ($C_i^*$) | Conclusion ($C_i^*$ = 1 is Ideal Solution) |
|---|---|---|
| Steel | 0.422164692 | |
| Aluminium | 0.486646985 | |
| E-Glass/Epoxy | 0.625015998 | Best Suited |
| Carbon/Epoxy | 0.593729557 | |
| Aramid/Epoxy | 0.573817216 | |

### C. Determination of Material Properties

Once the optimum material is selected for the blade, its properties must be obtained. The amount of information required about a material depends on the type and level of analysis [27]. For the current work, in order to perform basic structural analysis, the composite layers are assumed to be perfectly bonded and transversely isotropic. The material properties for static condition are determined by rule of mixtures and elastic approach models for a fiber volume fraction of 52 % [28], [29].

TABLE III
ELASTIC PROPERTIES OF E-GLASS/EPOXY MATERIAL FOR $V_F$ = 52%

| $\int$ | $E_{11}$ | $E_{22} = E_{33}$ | $v_{12}$ |
|---|---|---|---|
| 1896.80 [kg/m³] | 39.07 [GPa] | 9.39 [GPa] | 0.26 |
| $G_{12}$ | $v_{23} = v_{13}$ | $G_{23} = G_{13}$ | |
| 3.75 [GPa] | 0.33 | 3.52 [GPa] | |

TABLE IV
ULTIMATE STRENGTHS OF E-GLASS/EPOXY MATERIAL FOR $V_F$ = 52%

| | | |
|---|---|---|
| Ultimate Tensile Strength in Longitudinal Direction [MPa] | $\sigma^T_{1ult}$ | 806.04 |
| Ultimate Compressive Strength in Longitudinal Direction [MPa] | $\sigma^C_{1ult}$ | 727.34 |
| Ultimate Tensile Strength in Transverse Direction [MPa] | $\sigma^T_{2ult}$ | 44.68 |
| Ultimate Compressive Strength in Transverse Direction [MPa] | $\sigma^C_{2ult}$ | 126.59 |
| Ultimate In plane Shear Strength [MPa] | $\tau_{12ult}$ | 84.39 |

The determined elastic and ultimate strength parameters are listed in Tables III and IV. The fatigue properties are obtained from MSU/DOE fatigue database for the wind turbine blade materials [30]. The data from the tests carried out as per ASTM standards at a stress ratio of R = 0.1 and fiber volume fraction $V_f$ = 52 % is assumed for the selected material which is shown in Table V.

World Academy of Science, Engineering and Technology
International Journal of Mechanical and Mechatronics Engineering
Vol:9, No:6, 2015

TABLE V
FATIGUE PROPERTIES OF E-GLASS/EPOXY LAMINATE OF $V_F$ = 52 % AT R=0.1
TESTS [30]

| Description | Material ID | UTS $S_u$ [MPa] | Two slope model SN curve parameters | |
|---|---|---|---|---|
| | | | A [MPa] | B |
| Spar Cap material | Spar Mixture | 764.97 | 894.2 | -0.1 |
| Blade skin and Shear web material | CDB200 Triax | 478 | 1542 | -0.113 |

*D. Modeling and Analysis of Non-Segmented Blade*

The particulars of developing a non-segmented blade by using available data and method adopted for performance evaluation as per IEC61400-23 standard are presented through following steps:

1. Determination of Blade Geometry and Structural Parameters

The length of the blade is the primary and essential parameter in the design of rotor blade which influences the entire design process. Griffin [2] showed that, the blades of lengths nearly 45.7 m to 48.4 m which are having a mass of 9000 kg to 12000 kg respectively, serves the transition point in terms of transportation cost and handling difficulties. Thus, for modeling an experimental blade model, a 3 MW wind turbine blade having a length of 47 m (rotor radius of 49.5 m) is considered.

The base line configuration of the test blade is modeled in par with the guidelines provided in literature for wind turbine blade design [2], [31]. The plan form referred for the current study is shown in Fig. 1.
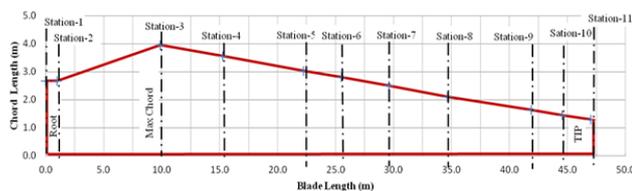


Fig. 1 Blade plan form

The test blade developed here closely resembles the configuration proposed by [33]. However, this should not be taken as a constraint against some necessary variation made during modeling. S818, S827 and S828 airfoils which are defined in particular for wind turbine applications are chosen to form the airfoil structure of the blade [32]. The developed blade consists of upper and lower spar caps with shear webs and their thickness varies along the span length with the chord. The exterior skins and internal shear webs have sandwich construction of composite laminate separated by balsa core. The spar cap comprises of composite layups with large number of uni-axial plies. Table VI shows the layup sequence used in the modeling of the blade.

TABLE VI
COMPOSITE LAYUP SEQUENCE USED FOR TEST BLADE [31], [33]

| Layer No. | Material | Layup | Thickness [mm] |
|---|---|---|---|
| Exterior Airfoil Skins | | | |
| 1 | Triax | [+45/-45/0]s | 1.27 |
| 2 | Balsa Core | ----------- | 0.005 x Chord Length |
| 3 | Triax | [+45/-45/0]s | 1.27 |
| Vertical Shear Webs | | | |
| 1 | Triax | [+45/-45/0]s | 1.27 |
| 2 | Balsa Core | ----------- | 0.01 x Chord Length |
| 3 | Triax | [+45/-45/0]s | 1.27 |
| Spar Caps | | | |
| 1 | Biax | [+45/-45] | 0.61 |
| 2 | Uniaxial | [0₂]s | 1.76 |
| Continued alternating layers of 1 and 2 | | | |

2. CAD Modeling

A non-segmented experimental wind turbine blade is modeled using CAD software CATIA V5 with estimated geometry parameters. The modeling of the blade helps in three dimensional visualization of its construction as in Fig. 2.
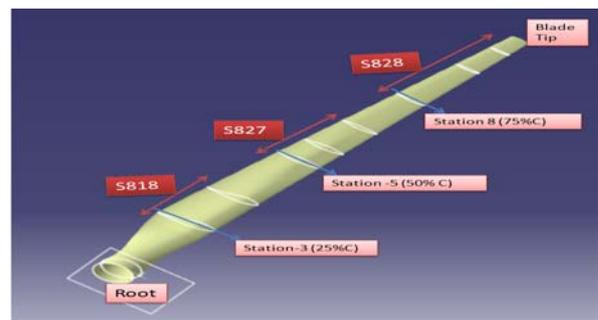


Fig. 2 CAD model of the test blade

3. Finite Element Modeling

The CAD model is imported into FEA tool ANSYS in IGES format and manually meshed with Solid46 element. Composite layers are modeled by using real constant setting mode. The gel coats, extra epoxy, and protective random mat layers are not modeled by assuming, they are not a part of load carrying members and to reduce the complexity in modeling. To arrive at optimum mesh size, the developed test blade is analyzed for a particular test load with different mesh sizes. The results obtained are shown in Fig. 3, which indicates that, an element with an area 200 mm² provide an optimum mesh. The size of the meshed model in terms of FEA is 96552 DOF's. The structure of an airfoil cross section at the maximum chord location with material layups is represented in Fig. 4.

4. Modal Analysis

The structural integrity and resonant characteristics play an important in the performance evaluation of wind turbine blades. Moreover, modal analysis is the preliminary step in structural analysis which provides the basic input towards segmentation. Hence, the non-segmented experimental blade is checked for its modal characteristics.
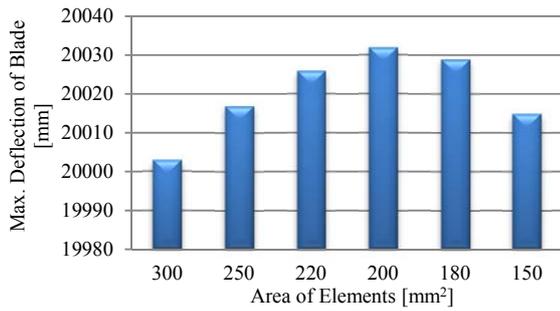
World Academy of Science, Engineering and Technology
International Journal of Mechanical and Mechatronics Engineering
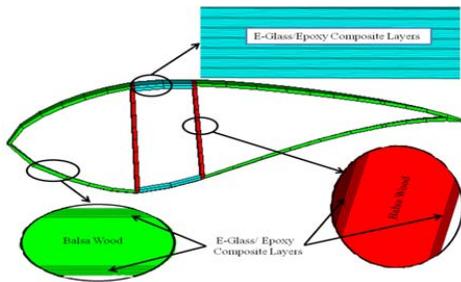Vol:9, No:6, 2015

Fig. 3 Mesh size optimization



Fig. 4 Cross section of meshed model showing material layups

To achieve the objective the base of the blade is fixed by constraining all DOF's for the nodes at the root section. The modal analysis is simulated by choosing Block Lancozos method and setting frequency range between 0 to 5Hz in ANSYS. The first six natural frequencies and mode shapes are extracted, and are recorded for reference to compare with that of segmented blade. The first mode shape is shown in Fig. 5.
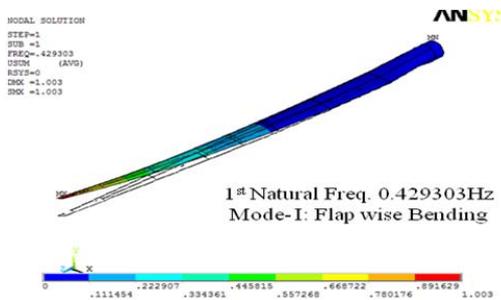


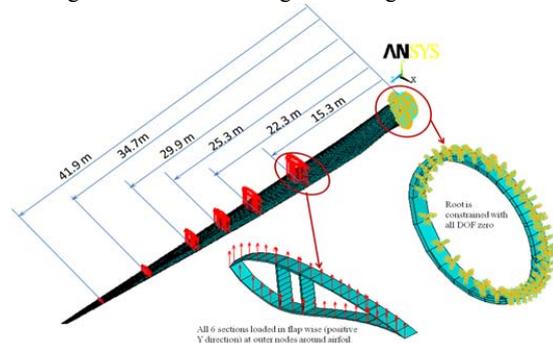Fig. 5 First mode bending of non-segmented blade



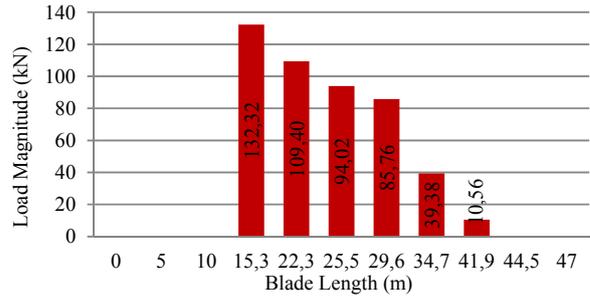Fig. 6 Non-segmented blade FE model with applied constraints



Fig. 7 Applied test loads for simulating static bending test [34]

5. Static Analysis

For simulating the static bending test, the blade is fixed at the root by constraining all degrees of freedom and a known magnitude of bending load is applied on the airfoil surface at 6 sections as shown in Fig. 6. The loads supposed here are from [34] and their magnitude is determined by scaling them appropriately with a non-dimensional scaling factor. Hence, they can be considered as representative loads. The magnitude of applied static bending test load is presented in Fig. 7.

A flap wise static bending test is simulated using FEA tool ANSYS in accordance with IEC61400-23 standard. The response of the blade is investigated in terms of displacements, stress and strains and is recorded to serve as reference for comparison with that of segmented blade. The change in deflection as a function of blade length is also estimated which helps in deciding suitable location for segmentation. The corresponding slope pattern is shown in Fig. 8 which does not exhibit any abrupt changes and clearly defines a region of linear behavior in the environs of mid span.
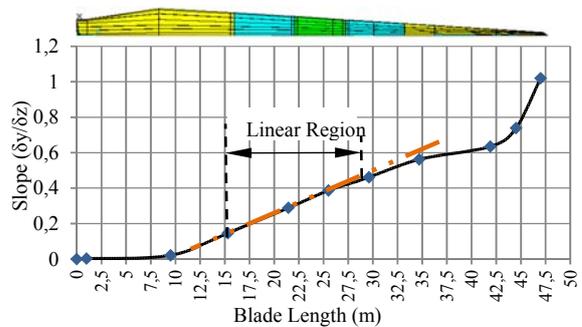


Fig. 8 Change in deflection v/s Length in non-segmented blade

6. Fatigue Analysis

The expected life of composite wind turbine blades is generally 20 to 25 years and experiences large number of varying loads during its service. These varying amplitude load sequences are often reduced to a constant amplitude block loading history to simplify the fatigue analysis. The flap wise fatigue load history used in this work is based on the study presented by [31], which is considered to be the representative load.

The fatigue analysis performed here is rather simplistic, since the material fatigue data for R=0.1 is assumed regardless of the individual load cycle R-value. A force displacement

World Academy of Science, Engineering and Technology
International Journal of Mechanical and Mechatronics Engineering
Vol:9, No:6, 2015

type of fatigue test is simulated for flap wise bending loads in accordance with IEC61400-23 standard through FEA tool ANSYS. The edgewise bending, axial, and torsion loads are not considered by assuming that, they are less severe than flap wise bending loads. The root is fully constrained by defining all DOF for the root nodes as zero. The maximum and minimum load amplitudes ($P_{max}$ and $P_{min}$) of every constant load block are applied alternatively on the airfoil cross section at 29.9 m location. The constant amplitude block loads used for the present analysis which give rise a cumulative of 7.65 x $10^8$ cycles is represented in Fig. 9.
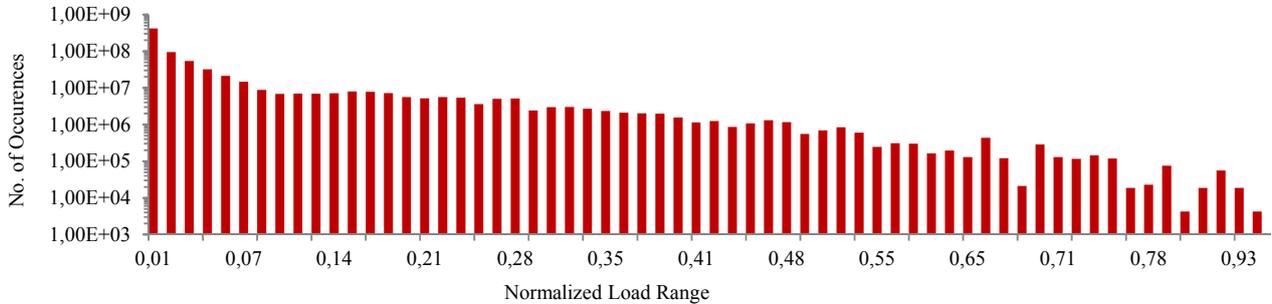


Fig. 9 Sample fatigue load spectra applied on the blade

The corresponding Von-Misses stresses ($\sigma_{Max}$ and $\sigma_{Min}$) developed in the blade are recorded and then, imported into a coded work sheet for fatigue damage estimation. This procedure is repeated for all 62 constant amplitude block loading cases using ANSYS batch run method. The critical regions identified for stress extraction for estimating fatigue damage are shown in Fig. 10.
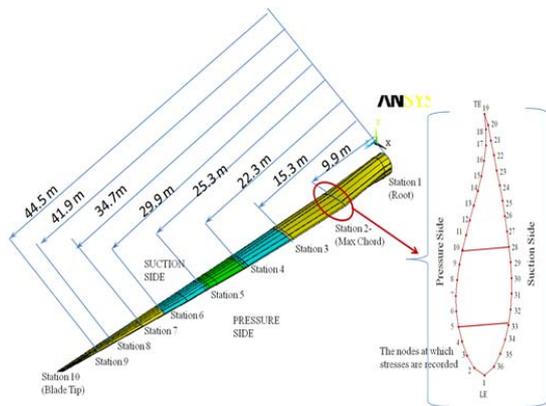


Fig. 10 Critical locations identified for fatigue damage estimation

Stress life approach is adopted in view of the fact that, it is sufficient to estimate the approximate fatigue life for the structures experiencing high cycle fatigue. Goodman criterion represented in (1) is used to account for mean stress effect by assuming E-glass/Epoxy composite has brittle behavior. However, this theory is developed for metals; we observed that, it is often used for accounting mean stress effects in composites due to non-availability of generalized efficient models and to reduce the complexity during analysis.

$$\frac{\sigma_a}{S_{NF}} + \frac{\sigma_m}{S_U} = 1 \qquad (1)$$

The cyclic stress amplitude and mean stress are calculated by using (2) and (3):

$$\sigma_a = (\sigma_{Max} - \sigma_{Min})/2 \qquad (2)$$

$$\sigma_m = (\sigma_{Max} + \sigma_{Min})/2 \qquad (3)$$

The equivalent numbers of cycles to failure are determined by using Basquin two slope fatigue model as in (4):

$$S = A\,(N)^B \qquad (4)$$

Finally, fatigue damage is estimated for critical sections by using Palmgren-Minor linear damage hypothesis as in (5):

$$Damage\ D = \left(\frac{n}{N_F}\right)_1 + \left(\frac{n}{N_F}\right)_2 + \left(\frac{n}{N_F}\right)_3 + \ldots\ldots\ldots + \left(\frac{n}{N_F}\right)_{61} + \left(\frac{n}{N_F}\right)_{62} \qquad (5)$$

This procedure is repeated to calculate the damage at every node around all identified cross sections (refer Fig. 10). The estimated damage in non-segmented blade is plotted as a function of blade length and width to serve as reference for comparison with that of segmented blade.

Fig. 11 depicts relatively low damage zone in the vicinity of mid span, which further depreciates along the length without any abrupt changes. A region of relatively large damage associated with high stresses is observed at the location of maximum chord.

Fig. 12 represents the fatigue damage variation around the airfoil sections at critical locations along the span from the root. At the location of maximum chord (9.9m section), relatively large damage is observed in the spar and shear web near the leading edge on pressure side due to large stress concentrations when compared with trailing edge. With the increase in length the location of maximum damage for each airfoil section shifts towards the trailing edge due to the twist in the blade which causes transition in stress concentration zone under applied loads.

World Academy of Science, Engineering and Technology
International Journal of Mechanical and Mechatronics Engineering
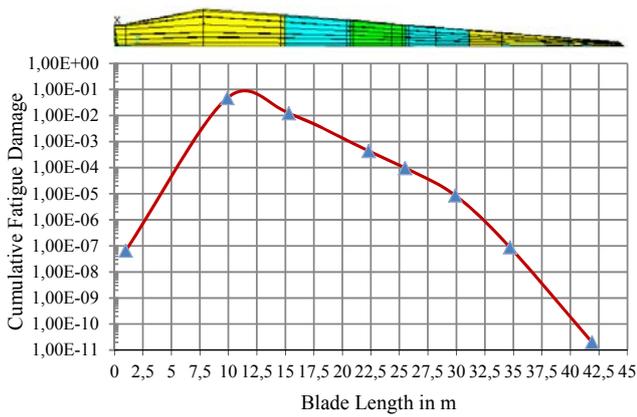Vol:9, No:6, 2015

Fig. 11 Maximum fatigue damage variations along the blade length
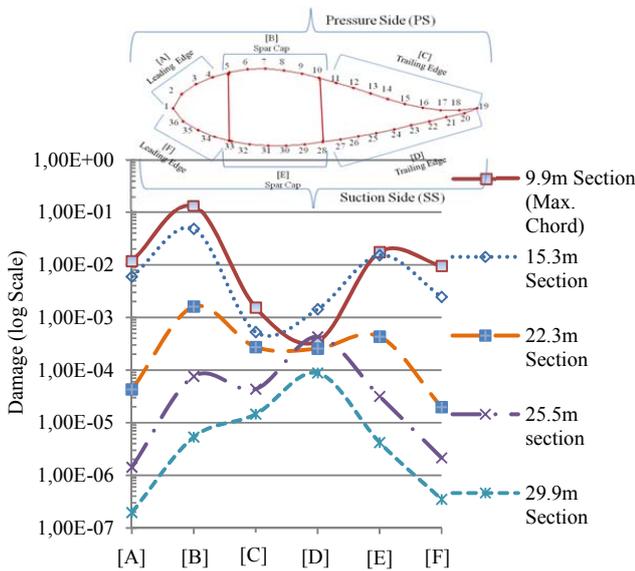


Fig. 12 Cumulative fatigue damage variations around cross sections

*E. Modeling and Analysis of Segmented Blade*

The process adopted for the modeling and performance evaluation of segmented blade is presented through following steps:

1. Identifying Suitable Location for Introducing Separation

The performance of a segmented blade greatly relies upon the effectiveness of the location selected for separation. Hence, the effort is to find an area rather than a single point/line which would provide an option of having more than one joint. The parameters considered for identifying the location are:

➢ Mode shapes of non-segmented blade.
➢ Change in deflection as a function of blade length for a non-segmented blade under static bending.
➢ Fatigue damage variation along the span length.
➢ Fatigue damage variation across the airfoil sections.

Mode shapes of non-segmented blade are analyzed for the modal bending behavior in order to identify an area with very

low deflection in the vicinity of nodal points. We observed that, it is not desirable to have a joint in the areas of large modal deflection which may lead to failure near resonance. The extracted mode shapes showed a region of negligible deflection up to mid span from the root (see Fig. 5). Towards the tip large deflections are observed which indicates separation cannot be provided beyond mid span. This gives a crude idea in deciding an area for segmentation which must be further supported with static bending and fatigue test results.

The static slope pattern for the non-segmented blade (see Fig. 8) and fatigue damage variation along the length (see Fig. 11) confirms that, separation can be provided in the region of mid span. However, for a wind turbine blade with two shear webs it is not desirable to have a separation at same location. This is to reduce the large stress concentration which may affect the joint strength. To distribute the joints over an area, the fatigue damage distribution across the cross sections in the vicinity of mid span is also studied (refer Fig. 12). We observed that, with the increase in length, the location of maximum damage for each airfoil section shifts towards the trailing edge due to the twist in the blade. This implies that, the joint on leading shear web must be provided away from the root and joint on the trailing shear web need to be relatively closer to the root within the identified region.

Further, the manufacturing constraints do influence the decision of selecting a suitable location for segmentation which requires separation at standard airfoil section. Hence, by considering the above, it is decided to have a separation in the vicinity of mid span with first joint on trailing shear web and the second joint on leading shear web at the location shown in Table VII.

TABLE VII
LOCATION IDENTIFIED FOR INTRODUCING SEPARATION

| Component | Leading Shear Web | Trailing Shear web | Airfoil blade shell |
|---|---|---|---|
| Distance from the root [mm] | 25500 | 22300 | 15300 and 29900 |

2. Selection and Design of Joint Configuration

The joint configuration considered here is based on [3], which identifies a double strap bonded joint as the most promising option among the considered alternatives. Also, to achieve a good bond it is necessary to select a good adhesive. In this study, an epoxy based structural adhesive HYSOL EA-9394 is considered, which is the most commonly used adhesive in wind turbine manufacturing and composite material industries [35], [36].

The potential failure modes for adhesively bonded joints considered are adhesion failure, cohesive failure of adhesive and tear failure of adherend. We assumed that, the selected adhesive has superior fatigue strength than adherends and hence, fatigue failure of adhesive is not considered as primary design constraint. Also, the variation in thickness of adhesive film is considered to be uniform and perfect bond between adherend and adhesive is assumed. The joint is designed and evaluated by a bonded joint design process in order to satisfy the requirement of developed test blade [37].

World Academy of Science, Engineering and Technology
International Journal of Mechanical and Mechatronics Engineering
Vol:9, No:6, 2015

### 3. Finite Element Modeling and Analysis

The existing FE model of the non-segmented blade is altered in the regions of separation to develop a segmented blade model. Metallic strap plates which have C-cross section geometry are incorporated at the joint as shown in Fig. 13.
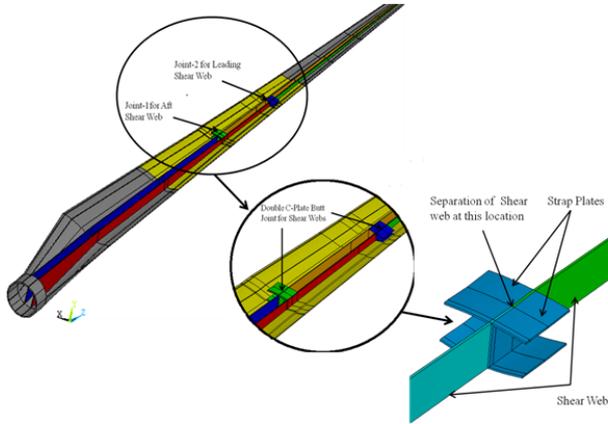


Fig. 13 Sectional View of developed segmented blade

The bonded joint configuration is modeled through Cohesive Zone Modeling (CZM) approach in ANSYS. In this method, the de-bonding is modeled as stiffness loss of the interface element based on a softening constitutive relation implemented in ANSYS software [38]. The interface surface is modeled by using special set of cohesive interface (contact) elements which are capable of simulating adhesive behavior. Bonded contact method is adopted since this method of representing contact and sliding surfaces is more compatible with layered SOLID46 element. CONTA174 a 3-D 8 noded surface to surface contact element is defined in association with TARGE170 3-D 8 noded target surface elements. Since fracture toughness is the measure of a material's ability to resist crack propagation, the material parameters required for simulating the adhesive behavior at joint are fracture test properties. The properties assumed here are from [36].

The developed FE model of the segmented blade has 19815 elements. The increase in number of elements when compared with non-segmented blade is observed due to meshing of strap plates and addition of contact elements. The structural integrity, load carrying capability and service life are estimated by simulating resonant, static bending and fatigue tests as per IEC61400-23 Standard. The load cases assumed and the methodology adopted for simulation is similar to that of non-segmented blade. The performance of the blade is recorded in terms of mode shapes, displacement, stress, strain, and cumulative damage for comparing with the reference.

## III. Results and Discussion

The performance of segmented blade is compared with that of non-segmented blade based on different parameters like, mass, resonant frequency, mode shapes, displacements, stress, and strains, and fatigue damage. The results of simulation are studied thoroughly through these performance parameters and detailed discussion is presented in following sections.

### A. Mass and Centre of Gravity of Developed Blade

The mass of non-segmented blade determined by partial solution method in ANSYS is found to be 13471 kg and mass of segmented blade as 13553kg. We observed that, the mass of segmented blade is increased by 82 kg due to the addition of four Al-2024 alloy strap plates at segmented regions. When checked for amount of displacement of center of gravity, it is found to be negligible for the blades in comparison. This shows that, segmentation did not affect the CG of the developed blade.

### B. Discussion on Modal Characteristics

Modal analysis of both the test blades is performed to check for any changes in physical parameters or boundary conditions. Their resonant behaviors are studied for the first six mode shapes and the following discussions are presented:

➢ The first resonant frequency found from simulation is 0.4293 Hz whereas the operating frequency determined, corresponding to the operating speeds is 0.2496 Hz. This indicates that, the developed test blades will not be subjected to resonance under normal operating conditions.

➢ For the blades in comparison, the natural frequencies and the corresponding mode shapes are found to be similar. This demonstrates that, segmentation did not affect the modal characteristics. A nominal deviation in magnitude of natural frequencies is observed due to addition of strap plates which resulted in increase in mass of segmented blade.

➢ We observed that, the structural integrity of the blade structure is unaffected even after segmentation. The deflections observed under modal bending are stable and no abrupt changes are found.

### C. Static Test Results

On application of bending load, the pressure side and the suction side of the blade is subjected to tension and compression respectively. It is the common behavior of structures subjected to bending where the outer and inner extreme layers experience tension and compression respectively, in the plane of bending. Hence, the layers on the pressure side of the blade are subjected to membrane effect and tend to slide past one another indicating a region of shear stress, popularly known as inter laminar shear stress, distributed between the layers in the vicinity of maximum chord. In segmented blade, the maximum shear stress is observed at the interface between shear web and strap plates due to sliding of the strap plates with the shear web.

From simulation results we observed that, a region of relatively high stress occurs near the root in both, segmented and non-segmented test blade due to large bending moments, which is the common characteristic of structures, treated as cantilever beam. It is necessary to check for the absolute value of this stress under the applied boundary conditions for better assessment of blade performance. Fig. 14 shows a region of maximum stress in the vicinity of maximum chord location

World Academy of Science, Engineering and Technology
International Journal of Mechanical and Mechatronics Engineering
Vol:9, No:6, 2015

(25 % R location) at the interface between the shear web and the blade shell. The high stress concentrations arising in this region are considered to be the effect of structural irregularities and an after effect of the damage initiation happened in the layers.
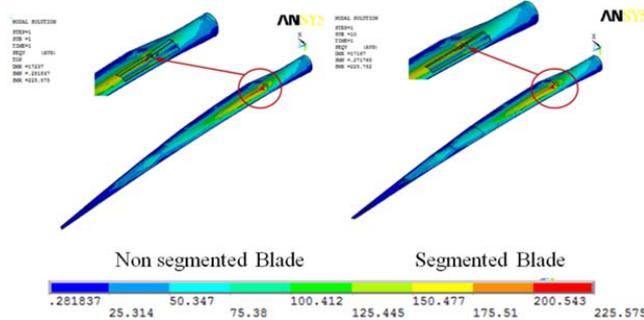


Fig. 14 Von-Misses stress distributions

In the areas of high stress concentration, it is essential to investigate the stress in each layer, to identify the damage initiation zone. The maximum stress concentration is observed in the layer 9 of the main load carrying member at the location of maximum chord length of the blade which is illustrated in Fig. 15. This layer is oriented along the blade axis and experiences a maximum stress of 225.75 MPa. The fiber alignment being orthogonal to the direction of loading, the matrix in this layer is contributing to the load carrying capability. Hence, matrix failure is the limiting criteria.

Under applied loads, this layer experiences shear deformation while surrounding layers of $45^0$ orientations tries to resist its motion, which causes high stress in the vicinity of this region. Investigation for the failure or damage of this layer is made by using Tsai-Wu and Tsai-Hill criteria which showed that, the composite is safe under applied static loads.
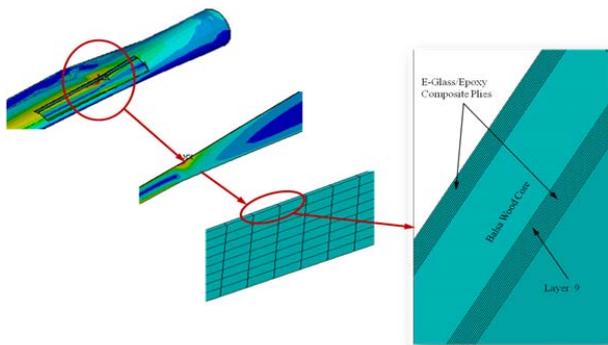


Fig. 15 Representation of layer of maximum stress

Since high levels of strains can produce damaging local distortions and high stress, all areas of segmented and non-segmented blade are examined to identify the maximum strain values and their location. As expected, the maximum strains are observed in the vicinity of maximum chord. The strain behaviors along and across the sections in both blades are found to be similar.
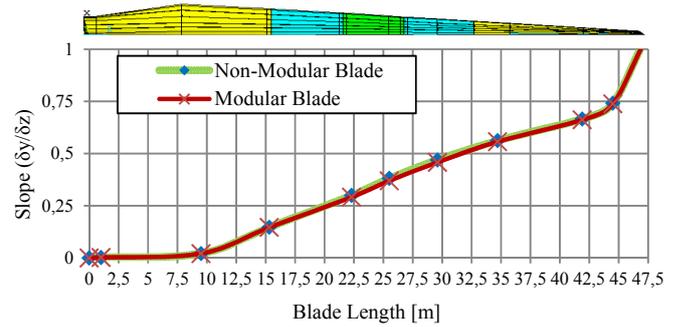


Fig. 16 Comparison of slope pattern in segmented and non-segmented blades

The slope pattern of the segmented and non-segmented blades, shown in Fig. 16 has no abrupt changes. The plot helps in evaluating the performance of blades in terms of deflection which is a direct measure of load carrying capability. We observed that, the slope of segmented blade is marginally lower than non-segmented blade due to the addition of Aluminum alloy strap plates which resulted in localized increase in blade stiffness. When checked for the percentage change in deflection, a maximum of 3 % change is observed in the vicinity of mid span which is a negligible quantity.

Thus, the static simulation results show that, segmentation did not affect the structural characteristics.

*D. Fatigue Test Results*

The graphical representation of the cumulative fatigue damage variation along the length for both the test blades is represented in Fig. 17. It is observed that, the linear fatigue damage variation is similar except a nominal increment in damage value in the vicinity of joints for segmented rotor blade. This increment in damage is considered to be the effect of stress concentrations arising due to discontinuity at the joints and variation in material stiffness caused by addition of metallic plates and adhesive for joining. The maximum damage in both the blades is found to be approximately equal to 0.1 at the location of maximum chord length (in the region of 9.9 m section) which is well away from the failure value of 1. Cumulative damage in all other regions is found to be relatively low and hence, both the blades are safe within assumed conditions. It is necessary to quantify the change in fatigue damage between the two blades in comparison for evaluating the effectiveness of segmented blade with that of non-segmented blade. The maximum rise in cumulative damage observed in the vicinity of joint 2 at 25.5m location in segmented blade is nearly 0.6% more than that of non-segmented blade which is a nominal quantity. No other abrupt damage fluctuations are observed and hence, the segmented test blade can be considered to have approximately equal life span as that of non-segmented rotor blade in comparison.
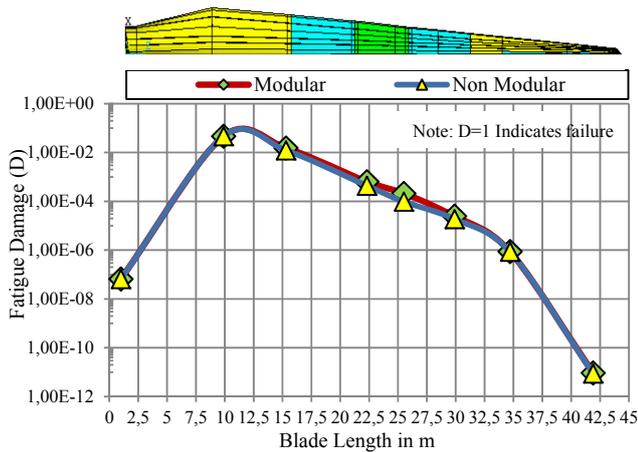
World Academy of Science, Engineering and Technology
International Journal of Mechanical and Mechatronics Engineering
Vol:9, No:6, 2015

Fig. 17 Comparison of maximum damage variations along blade span
in segmented and non–segmented blade

Fatigue damage variations around the circumference of airfoils at critical regions, is also investigated for understanding the effect of joint on damage distribution. We noted that, in the sections near to the root, larger damage exists on the pressure side since; the dominant tensile forces are more severe than compressive forces on the suction side. When location of cross sections is considered as function of length it is seen that, the larger magnitude of damage shifts from the leading edge towards the trailing edge. This is believed to be the effect of pre-twist in the blade which creates large stress zones towards the trailing edge with increase in length.

It is also noted that, the damage diminishes along the length which indicates lower stress levels in the sections farther from fixed end. All the critical regions of segmented test blade are thoroughly checked for its performance under fatigue load by comparing with non-segmented blade. The results showed comparable and acceptable performance.

### E. Cohesive Zone Model Results at Joints

The reliability and structural integrity of segmented blade relies upon the adequate bond between its composite shear web and aluminum alloy strap plates. In order to achieve safe design, it is very much essential to understand the behavior of the adhesive and strap plates under the applied loads along with the full structural response of the segmented blade.

On application of the load, the edges of the strap plates are impinging onto the surface of the blade shell which causes a region of high localized adhesive contact stresses at the edges as shown in Fig. 18. This behavior is considered to be the effect of difference in stiffness of metallic plates and composite blade shell.
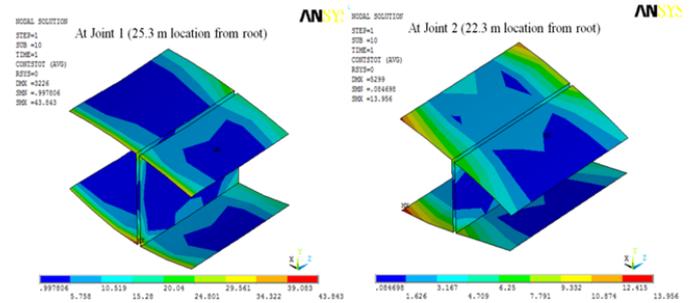


Fig. 18 Adhesive contact stress distribution

The stress variation in strap plates at both the joints is studied since it affects the efficiency of the joint and thus, the structural integrity of segmented blade. At joint 1, a region of high stress concentration is observed at the location of blade shell and plate interface due to the high pressure on the blade shell as shown in Fig. 19. At the Joint 2, the plates are subjected to bending which generates relatively high stress at the center. The failure assessment for the strap plates is carried out by using Distortion Energy Theory and found that, the strap plates are safe under applied loads. Moreover, the results obtained for joints are also compared with [3], and are found to be similar. The deviation observed in magnitude of displacement, stress and strains can be accounted for the variation in blade size, geometry, structure and materials. This indicates that, the adopted joint configuration can be a viable option, even for large size blades manufactured with different materials.
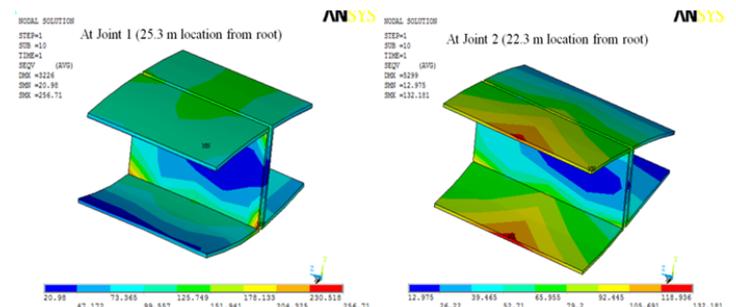


Fig. 19 Von-Misses stress distribution in strap plates

### IV. CONCLUSION

In this work, an attempt is made to develop a segmented wind turbine blade and test its structural performance through finite element simulation. The results indicate that, the effect of segmentation on the overall structural performance is minimal. Developed segmented blade appears to be the feasible alternative considering its structural response specifically in fatigue within considered assumptions. The method adopted to locate the region for segmentation has proved to be effective. Thus, the basic objective of developing a potential segmented wind turbine blade which shows similar performance as that of non-segmented blade is achieved.

REFERENCES

[1] "Design limits and solutions for very large wind turbines," UPWIND, EWEA, pp. 10-18, March 2011.

[2] D. A. Griffin, "Blade System Design Studies Volume I: Composite Technologies for Large Wind," SANDIA National Laboratories, California, USA, 2002.

[3] F. A. Saldanha, V. V. Rao, J. Chirstopher and R. Adhikari, "Investigations on concepts for modularizing a horizontal axis wind turbine blade," in Proceedings of the ASME 2013 IDETC/CIE Conferences, Portland, Oregon, Aug 4-7, 2013.

[4] MEGAWIND, "30m split rotor blade," (Online). Available: http://www.cres.gr/megawind.

[5] P. Vionis, D. Lekou, F. Gonzalez and Others, "Development of a MW scale wind turbine for high wind complex terrain sites; the MEGAWIND Project," in Proceedings of EWEC conference on Innovative turbines, components, systems and techniques, Athens, March 2006.

[6] Paul W. Judge, "Segmented Wind turbine Blade". US Patent US7854594B2, December 21, 2010.

[7] Enno Eyb, "Modular rotor blade for a wind turbine and methods for assembling same". US Patent US20070253824 A1, Nov 1, 2007.

[8] M. L. Baker and C. P. Arelldt, "Lightweight composite truss wind turbine blade". US Patent US7517198 B2, 14 April 2009.

[9] P. T. Hayden and P. A. Broome, "Wind Turbine Blade". US Patent US20110103962 A1, 5 May 2011.

[10] D. J. Kootstra, "Wind Turbine Rotor Blade Joint". US Patent US8172539 B2, MAY 8, 2012.

[11] J. Stege, "Wind turbine rotor blade". Europe Patent EP2749765A1, July 2, 2014.

[12] "Modular design eases big wind blade build," COMPOSITES, August 2013.

[13] J. Broehl, "Wind Energy Innovations: Segmented Blades," 4 August 2014. (Online). Available: http://www.navigantresearch.com/blog/.

[14] S. N. Ganeriwala and M. Richardson, "Modes indicate cracks in wind turbine blade," in 29th IMAC Conference, Jacksonville, FL, 2011.

[15] H. B. Pederson and O. J. Kristensen, "Applied modal analysis of wind turbine blades," Riso National Laboratory, Denmark, February 2003, ISBN: 87-550-3170-6.

[16] G. C. Larsen, M. H. Hansen, A. Baumgart and I. Carlen, "Modal analysis of wind turbine blade," Riso National Laboratory, Denmark, February 2002, ISBN: 87-550-2697-4.

[17] F. Fors and T. Mekanik, "Analysis of metal to composite adhesive joints in space applications" MS thesis, Linkoping University, Sweden, 2010.

[18] V. A. Kalkhoran, D. S. Majd and B. Mohammadi, "Fatigue Life Prediction for Adhesively Bonded Root Joint of Composite Wind Turbine Blade Using Cohesive Zone Approach," Conference of Recent Advances in Composite Materials for Wind Turbines Blades, The World Academic Publishing Co. Ltd., 2013, pp. 221-231, ISBN 978-0 9889190-0-6, Available at: http://www.academicpub.org/amsa.

[19] Eric Hau, Wind Turbines: Fundamentals, Technologies, Application, Economics, 2nd ed., Germany: Springer, 2006.

[20] A. R. Jha, Wind Turbine Tecnology, 1st ed., NewYork: CRC Press, 2011.

[21] Guidelines for Design of Wind Turbine, 2nd ed., Denmark: DNV and RISO National Laboratories, 2002.

[22] K. Vallons, G. Adolphs, P. Lucas and S. V. Lomov, "Quasi-UD glass fibre NCF composites for wind energy applications: a review of requirements and existing fatigue data for blade materials," Journal of Mechanics and Industry, vol. 14, pp. 175-189, 2013.

[23] IEC-TS64100-23, Wind turbine generator systems –Part 23:Full-scale structural testing of rotor blades, 1st ed., International Electrotechnical Commission, 2001.

[24] S. K. Babu, N. V. Subbaraju, S. M. Reddy and N. D. Rao, "The material selection for typical wind turbine blades, using MADM approach and analysis of blades," in Conference on Multiple criteria decision making, Chania, Greece, June 19-23, 2006.

[25] H. J. Sutherland, "A Summary of the Fatigue Properties of Wind Turbine Materials," Wind Energy, vol. 3, pp. 1-34, 2000.

[26] P. J. Schubel and R. J. Crossley, "Wind Turbine Blade Design," Energies, vol. 5, pp. 3425-3449, 2012.

[27] Peter Robert Greaves, "Fatigue Analysis and Testing of Wind Turbine Blades, Durham Thesis," Durham University, Durham, UK, May 2013.

[28] R. M. Jhones, Mechanics of composite materials, 2nd ed., Philadelphia: Taylor and Francis, 1999, ISBN: 1-56032-712-X.

[29] K. Kaw, Mechanics of composite materials, 2nd ed., Taylor and Francis, 2006.

[30] DOE/MSU Composite Material Fatigue Database, Version 18.1, US, March 25, 2009.

[31] D. A. Griffin, "Blade System Design Studies Volume II: Preliminary Blade Designs and Recommended Test Matrix," SANDIA National Laboratories, California, USA, June, 2004.

[32] "Airfoil coordinates," (Online). Available: http://www.nrel.gov.

[33] D. T. Griffith and T. D. Ashwill, "The Sandia 100-meter All-glass Baseline Wind Turbine Blade, SANDIA Report," SANDIA National Laboratories, California, USA, June, 2011.

[34] F. M. Jensen, "Ultimate strength of a large wind turbine blade, Risø-PhD-34(EN)," Riso National Laboratories and DTU, Denmark, May, 2008.

[35] Hysol-EA 9394: Epoxy Paste Adhesive Catalogue, CA, USA: Henkel Corporation, Available At: www.aerospace.henkel.com.

[36] F. Fors and T. Mekanik, "Analysis of metal to composite adhesive joints in space applications" MS thesis, Linkoping University, Sweden, 2010.

[37] J. L. C. (Ed.), EUROCOMP Design Code and Handbook: Structural Design of Polymer Composites, Chapman and Hall, 2005, ISBN: 0-203-47513-5.

[38] ANSYS V14 User Manual, ANSYS Inc.